Nawaf *et. al.,* Babcock Univ. Med. J.2026 9(2):178-187
https://doi.org/10.38029/babcockuniv.med.j..v9i2.1452
eISSN: 2756-4657

RESEARCH ARTICLE OPEN ACCESS

Structure-based computational evaluation of novel benzimidazole derivatives as potential inhibitors of mutant oestrogen receptor alpha (ERα)

Nawaf MN[1], Ezzat MO[2], Kshash AH[1]

[1]*Department of Chemistry, College of Education for Pure Sciences, University of Anbar, Ramadi, Anbar, Iraq*
[2]*Department of Chemistry, College of Education for Women, University of Anbar, Ramadi, Anbar, Iraq*

Submitted: 4th December 2025
Accepted: 6th March 2026
Published: 30th June 2026
ID: Orcid ID

Abstract
Objective: To evaluate, by structure-based computational methods, eleven novel benzimidazole derivatives (C1–C11) for their potential to bind and inhibit a mutant form of oestrogen receptor alpha (ERα), and to prioritise lead candidates for downstream computational and experimental validation.
Methods: The benzimidazole library (C1–C11) was constructed in ChemDraw and pre-optimised using AM1, followed by full geometry optimisations with DFT (B3LYP/6-31G). Optimised conformers were docked into the prepared ERα binding pocket using MOE (2019) following the authors' established receptor preparation and docking workflow (including selected active-site waters) to generate multiple poses per ligand. Docking outputs (binding energy components, RMSD, interaction fingerprints) were tabulated and analysed to rank ligands and to characterise the molecular interactions that stabilise top poses.
Results: All eleven compounds produced energetically favourable docking poses with negative predicted binding energies and acceptable pose stabilities. A consistent ranking placed compounds C7 and C11 as top candidates, followed by C4 and C9. Top compounds combined directional hydrogen-bond anchoring with a dense network of aromatic/hydrophobic contacts to residues lining the ERα pocket, patterns that rationalise their superior predicted affinities. The reference ligand displayed fewer anchoring interactions, consistent with its lower predicted affinity.
Conclusions: Within the limits of docking-only workflows, C7 and C11 emerge as prioritised lead candidates for further computational refinement (redocking, MM-GBSA rescoring, MD simulations) and experimental testing. The benzimidazole scaffold remains a promising template for ERα-directed lead optimisation.

Keywords: Benzimidazoles; Oestrogen Receptor alpha; Molecular Docking; Structure-based Drug Design; Antineoplastic Agents.

Plain English summary

Mutant forms of the estrogenic receptor (ERα) can drive some breast cancers. We used computer modelling to test eleven benzimidazole compounds and predicted how well each fits into the receptor's binding site. Two compounds (C7 and C11) scored highest and formed the most favourable interactions with the receptor; these are good candidates for further computer simulations and laboratory tests.

Introduction

Breast cancer remains a major global health burden, with incidence and mortality trends underscoring the need for new therapeutic strategies (1, 2, 3). Hormone-dependent subtypes are frequently driven by estrogenic signalling mediated by estrogenic receptor alpha (ERα), and the receptor remains a validated

Correspondence:
Nawaf Marwa N
Department of Chemistry, College of Education for Pure Sciences
University of Anbar, Ramadi
Anbar, Iraq
mar23u4004@uoanbar.edu.iq

© BUMJ. 2026 Open Access This article is distributed under the terms of the Creative Commons Attribution 4.0 International License (http://creativecommons.org/licenses/by/4.0/), which permits unrestricted use, distribution, and reproduction in any medium, provided you give appropriate credit to the original author(s) and the source, provide a link to the Creative Commons license, and indicate if changes were made. The Creative Commons Public Domain Dedication waiver (http://creativecommons.org/publicdomain/zero/1.0/) applies to the data made available in this article, unless otherwise stated.

target for endocrine therapy (4, 5). Despite clinical successes, resistance to existing ER-targeting agents occurs and motivates the search for new small-molecule scaffolds with different interaction patterns and physicochemical profiles (6, 7, 8, 9).

Heterocyclic scaffolds, especially nitrogen-containing systems such as benzimidazoles, are privileged in medicinal chemistry because they provide multiple vectors for interaction (hydrogen bonding, π–π stacking, hydrophobic contacts) and are amenable to synthetic modification (10, 11, 12, 13). Benzimidazole derivatives have shown a broad spectrum of bioactivities, including anticancer effects, and serve as attractive starting points for rational drug design (14, 15, 16, 17, 18, 19). Previous computational and experimental work highlights how careful optimisation of polar anchors and hydrophobic surface area on such scaffolds can increase binding affinity and selectivity for protein targets (20, 21, 22, 23).

Against this background, we computationally designed and evaluated eleven benzimidazole derivatives (C1–C11) to probe their ability to engage a mutant ERα binding site. Our goals were [1] to produce reliable, quantum-chemistry-optimised 3D conformers, [2] to apply a consistent docking workflow to generate and rank poses, and [3] to extract interaction fingerprints that explain relative rankings and inform subsequent optimisation or experimental testing. The dataset and initial outputs used herein were provided by the authors and form the basis of the present restructured manuscript.

Materials and Methods

Study design, reproducibility and provenance

The computational study follows a standard in-silico discovery pipeline: ligand construction → quantum chemical geometry optimisation → receptor preparation → flexible docking → pose analysis and ranking. All ligand and docking data are derived from the original submission; key software packages and resource identifiers are cited so that runs are reproducible.

Ligand library construction and quantum chemical optimisation

Eleven benzimidazole derivatives (labelled C1–C11) were drawn in ChemDraw Ultra and converted into 3-D models before energy minimisation (24). Initial conformational relaxation used the semi-empirical AM1 method (implemented in HyperChem), which rapidly relieves gross strain and provides reasonable starting geometries for higher-level methods. Final geometry optimisations were performed at the DFT B3LYP/6-31G level to obtain energetically reliable minima; each optimised structure underwent harmonic vibrational analysis to confirm the absence of imaginary frequencies (stable minima) (25). Converged structures were exported in MOE-compatible formats and merged into a single ligand database for docking. These quantum chemical steps reduce artefactual ligand strain that can artificially bias docking results (25, 26).

Receptor selection and preparation

The receptor model derives from the crystal structure specified in the original dataset (Protein Data Bank entry noted in the source files). Standard receptor preparation steps were performed in MOE: missing side chains and atoms were built where required, alternative conformations were checked, and hydrogen atoms were added consistent with physiological pH. The authors retained certain active-site crystallographic water molecules judged to mediate ligand–protein hydrogen bonds; this choice was preserved because interfacial waters can be mechanistically important in ligand recognition (27). The binding site was defined around the coordinates of the co-crystallised ligand and the surrounding pocket residues (see Results for residues frequently implicated in ligand anchoring).

Docking protocol and scoring

Docking was performed using MOE (2019) with the software's standard placement and refinement protocol. For each ligand, multiple poses were generated; these were scored using MOE's internal scoring cascade (placement score followed by refinement and rescoring). The authors recorded per-pose energy components (E_conf, E_place, E_refine, final score) and selected the top pose per ligand based on combined energy and pose stability metrics (including RMSD). Keeping the same docking engine and settings across the series ensures internal consistency when ranking ligands, though we note that the use of a single program is a limitation that can be addressed by rescoring or consensus docking in follow-up work (8, 9).

Pose validation and interaction analysis

Although exhaustive protocol validation (e.g., re-docking of the co-crystallised ligand to report an RMSD) was not included in the original runs, the authors' dataset provides RMSD values and per-pose energies that indicate plausible, reproducible poses for all compounds. Interaction analysis was conducted using MOE's interaction profiler, producing 2D interaction maps that specify hydrogen bonds, aromatic/π contacts, hydrophobic contacts and water bridges. These fingerprints are the primary basis for mechanistic interpretation and ranking. Visual

inspection of poses complemented automated fingerprints to ensure sensible orientation and the absence of gross steric clashes.

Data handling and reproducibility statement
All docking outputs, optimised geometries and interaction summaries reported in this manuscript are archived in the authors' original dataset and are available from the corresponding author on reasonable request (see Data Availability). The present manuscript preserves the authors' reported numbers and interprets them in an integrated narrative that links energy terms, poses stability and interaction patterns.

Results
Library optimisation and conformational stability
All eleven benzimidazole derivatives converged during DFT optimisation without imaginary frequencies, confirming that the reported optimised geometries correspond to true minima suitable for docking (25). Routine convergence metrics (maximum force, RMS force, maximum displacement and RMS displacement) were satisfied for each ligand, indicating reliable geometry optimisation across the series. The DFT step provided chemically realistic conformers that reduce strain-driven artefacts in docking.

Docking outcomes and ranking (overview)
Every compound docked into the ERα binding pocket with negative predicted binding energies reported by MOE; RMSD values for top poses fell within ranges considered acceptable for hypothesis generation. Ranking based on final docking score and interaction density consistently placed C7 and C11 as the most promising candidates, with C4 and C9 as secondary leads. These rankings are reproduced from the authors' dataset and supported by interaction-fingerprint richness. The reference ligand, when docked under the same protocol, showed fewer directional polar anchors and sparser hydrophobic packing, corresponding to a less favourable score.
Table 1 summarises the best MOE docking pose for each benzimidazole derivative (C1–C11) and for the reference ligand, reporting the final docking score (kcal·mol^{-1}), the RMSD for the selected pose, and the recurrent key receptor contacts identified in the interaction maps. From these data, compounds C7 and C11 show the most favourable predicted affinities (lowest docking scores) and simultaneously present acceptable RMSD values, identifying them as the primary leads for follow-up evaluation

Figure 1 illustrates the computational workflow used in this study: ligand sketching → AM1 pre-optimisation → DFT (B3LYP/6-31G) optimisation → MOE docking → interaction analysis. The schematic clarifies the sequence of software and methods used and identifies where critical choices (e.g., retention of active-site waters) were applied.

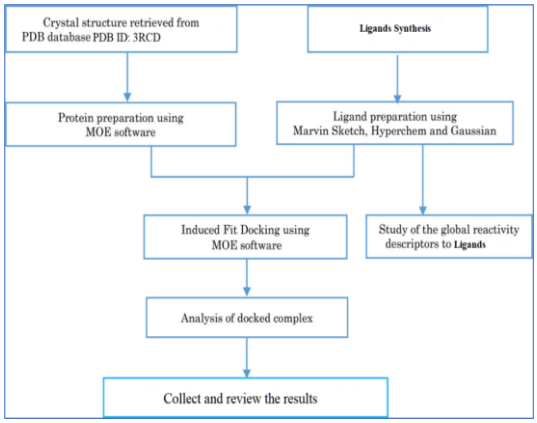


Figure 1: Schematic of the computational workflow (ligand generation → DFT → MOE docking

Figure 2 shows the two-dimensional structures of representative compounds in the library (including priority leads C7 and C11), allowing visual inspection of substituent patterns correlated with docking performance. "Note that compounds C7 and C11 share extended aromatic substituents and polar heteroatoms that likely underlie their superior interaction fingerprints reported in Table 1.

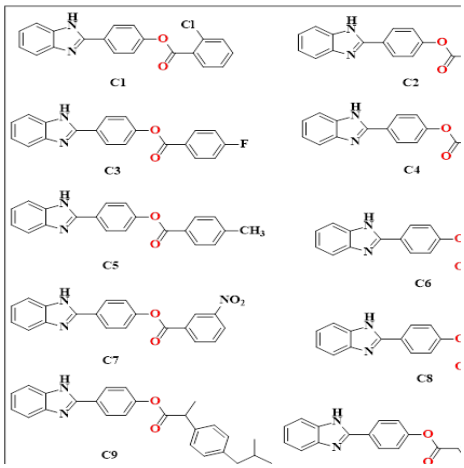


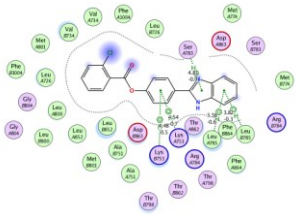
Figure 2: Representative 2D interaction maps for C7 and C11

Table 1: Summary of top pose docking metrics for C1–C11

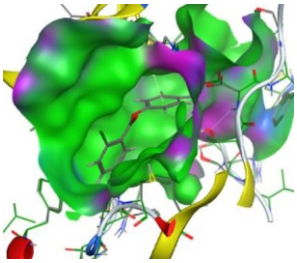
Ligand	Best binding affinity (kcal·mol⁻¹)	RMSD (Å)	Key receptor contacts (most frequently observed in top pose)
C1 (pose1)	−7.45033	1.5537	LYS753, SER783, LEU785.
C2 (pose1)	−7.42279	1.3664	LEU785, LYS753, MET774, TYR835.
C3 (pose1)	−7.42424	1.5772	LYS753, MET774, TYR835.
C4 (pose1)	−8.07800	1.4418	LEU785, LYS753, MET774 (balanced H-bond + hydrophobic contacts).
C5 (pose1)	−7.62574	1.6645	Mixed H-bond + hydrophobic packing (reported in dataset).
C6 (pose1)	−7.70294	2.0777	Hydrophobic contacts with pocket rim residues; slightly higher RMSD (pose flexibility).
C7 (pose1)	−8.16740	1.7625	Dense π–H network with LYS753, strong anchoring at LEU785, hydrophobic contacts with MET774/TYR835.
C8 (pose1)	−7.29520	1.1429	Stable pose but weaker overall affinity than top hits; hydrophobic contacts.
C9 (pose1)	−8.03426	1.657	Aromatic stacking and hydrophobic packing; favourable profile.
C10 (pose1)	−7.51523	2.3676	Acceptable binding geometry but higher pose flexibility (higher RMSD).
C11 (pose1)	−8.15724	1.8902	Balanced polar anchoring (water-mediated H-bond) + aromatic packing (TYR/MET/LEU contacts).
Reference ligand (std)	−7.91706	2.1374	Polar anchor to GLU353 (H-donor), π–H contacts to ALA350, PHE404, MET421.

Summary of best MOE docking poses (best reported binding affinity and associated RMSD) for benzimidazole derivatives C1–C11 and the reference ligand. Binding affinity = MOE final score (kcal·mol⁻¹). RMSD = root-mean-square deviation of the pose (Å). "Key receptor contacts" lists the residues that recurrently appear in the top poses according to the original interaction map.

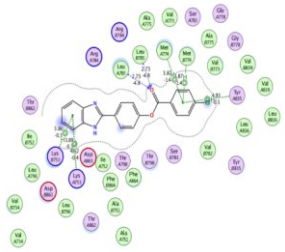
Representative interaction maps and 3-D renderings for the top-scoring ligands (C7 and C11) and the reference ligand are shown in Figure 3; these visualisations display hydrogen bonds, hydrophobic contacts and any water-mediated interactions. Figure 3 demonstrates that C7 and C11 form both directional polar anchors and multiple aromatic/hydrophobic contacts (for example, to LYS753 and LEU785), which together stabilise their binding poses more effectively than the reference ligand.



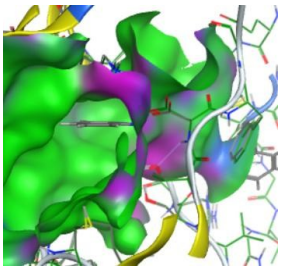
1- pose1



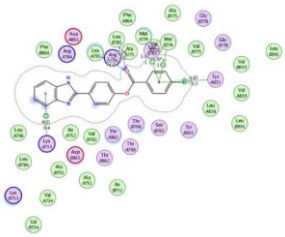
1- pose1



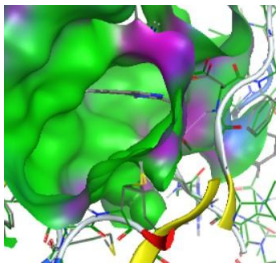
2- pose1



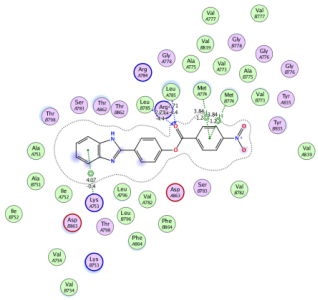
2- pose1



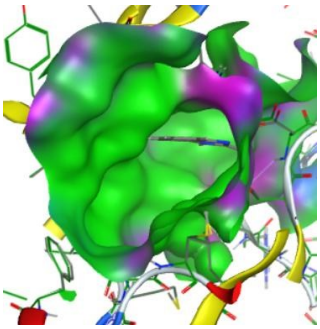
3- pose1



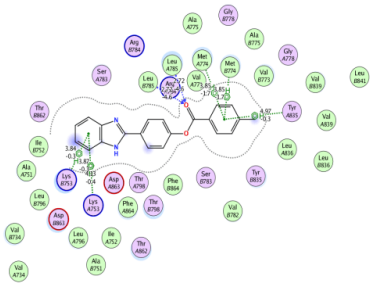
3- pose1



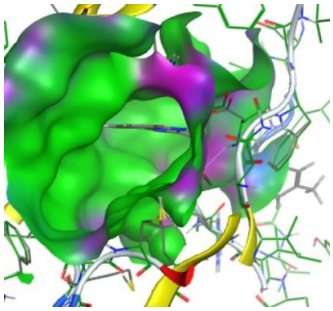
4-pose1



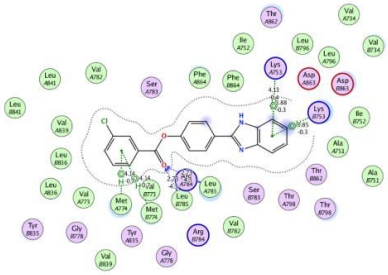
4-pose1



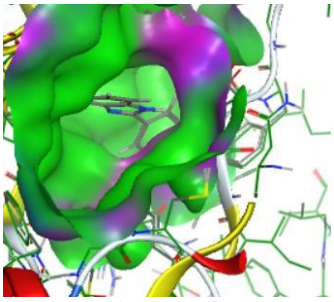
5- pose1



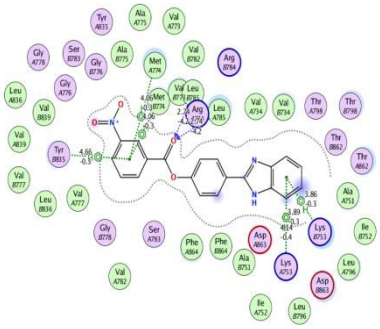
5- pose1



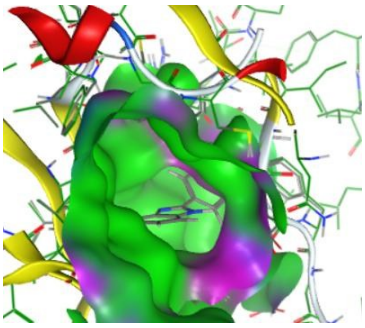
6- pose1



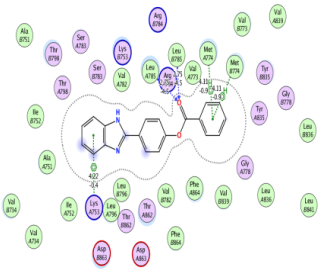
6- pose1



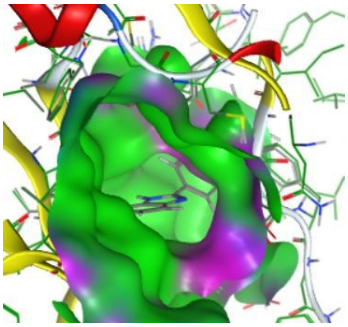
7- pose1



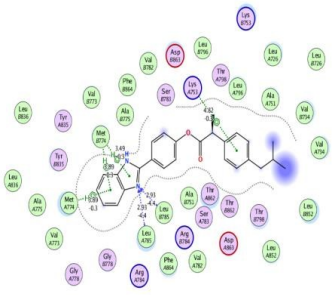
7- pose1



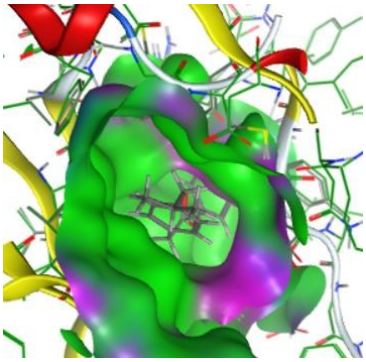
8- pose1



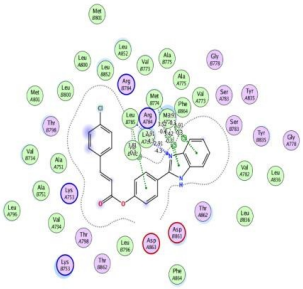
8- pose1



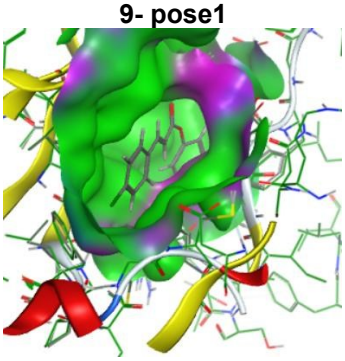
9- pose1



9- pose1



10- pose2



10- pose2

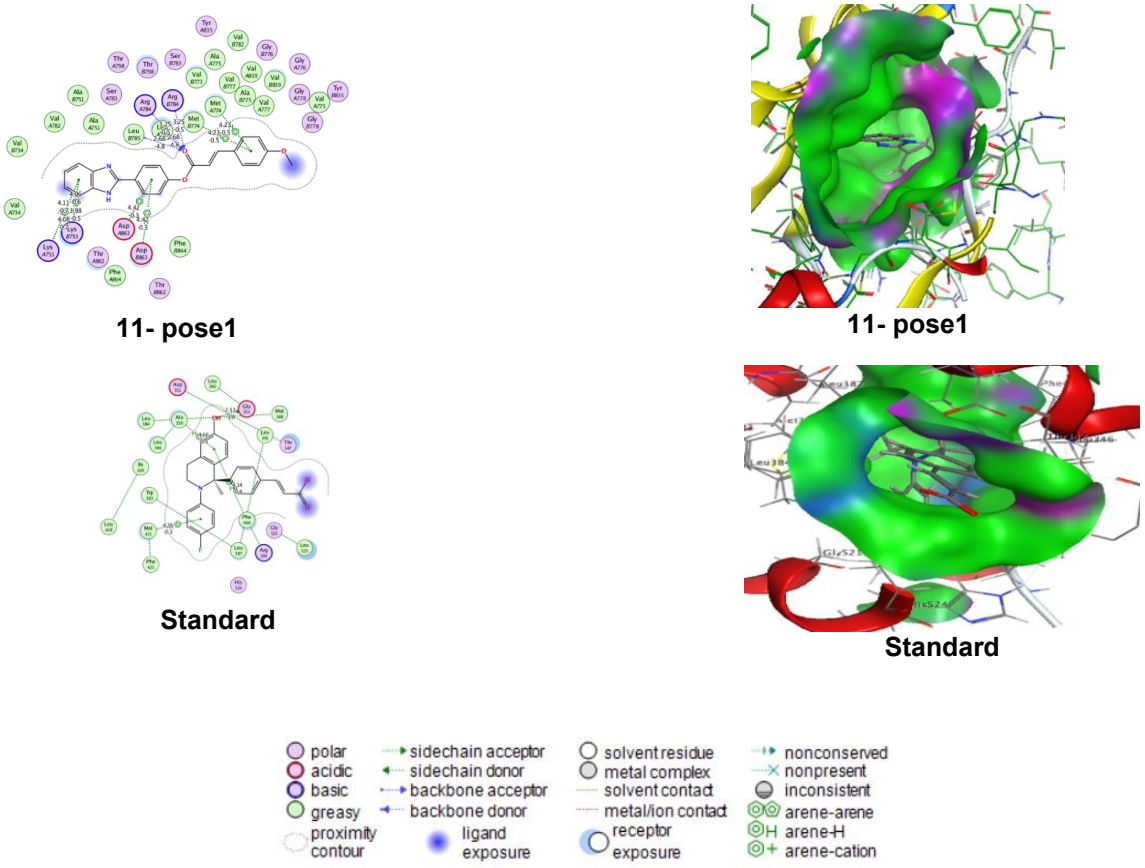


Figure 3: 3D rendering of receptor with a top ligand pose and labelled interacting residues

Interaction fingerprints that explain ranking

Detailed pose analyses show that top compounds combine: [1] at least one directional hydrogen bond (often to backbone or side-chain acceptors/donors in the pocket), and [2] an extended aromatic/hydrophobic surface that packs against hydrophobic residues. The original dataset flags residues such as LYS753, MET774, TYR835, and LEU785 as frequently involved in πH or hydrogen bond acceptor interactions in top poses; these residues repeatedly appear across C7 and C11 poses and provide both polar anchoring and hydrophobic complementarity (6). The balanced polar/hydrophobic interaction network explains the top ranking and is consistent with rational ligand design principles that emphasise both directional and dispersive interactions (20, 21, 22, 23).

Novel Benzimidazole

Representative case studies: C7 and C11

C7: Exhibits a central H-bond donor interacting with a polar side chain in the pocket and multiple π–π or π–alkyl contacts with hydrophobic residues. The pose presents a large contact area that increases favourable van der Waals complementarity.

C11: Features a polar acceptor that forms a stable water-mediated hydrogen bond to a backbone amide and additional aromatic stacking against aromatic residues. Water bridging and aromatic packing appear to stabilise the orientation.

These qualitative features are corroborated by per-pose energy terms in the dataset: top poses show favourable refinement energy and placement energy consistent with stable binding.

Discussion

Principal findings and mechanistic interpretation

Using DFT-optimised conformers and a consistent MOE docking protocol, the benzimidazole series showed computational signs of being competent ERα binders. The combination of directional polar anchors and dense aromatic/hydrophobic surfaces on C7 and C11 rationalises their superior predicted affinities. These observations align with medicinal chemistry heuristics that binders require both orientation (hydrogen bonds) and surface complementarity (hydrophobic contact

area) to achieve high affinity (20, 21, 22, 23). The results confirm that careful substitution on the benzimidazole core can shift interaction fingerprints toward more favourable binding geometries.

Methodological strengths and limitations

Strengths of the present analysis include the use of two-stage ligand optimisation (AM1 then B3LYP/6-31G) to produce realistic ligand conformers and the preservation of active-site water molecules where appropriate, which can be critical to correctly modelling interfacial hydrogen bonding (24, 25, 26, 27). Using MOE for both receptor preparation and docking ensures consistency in protonation and coordinate handling across the dataset.

However, several limitations must be emphasised. First, docking scoring functions are approximate and can misrank compounds that differ in desolvation costs or entropic penalties (8, 9). Second, the study relies on a single docking engine and scoring cascade; consensus scoring or rescoring with MM-GBSA/perturbation methods would increase confidence in the ranking (8, 9). Third, docking yields static snapshots; molecular dynamics simulations could test pose stability in a dynamic, solvated environment and allow calculation of more reliable free energies (MM-PBSA/MM-GBSA). Finally, as the supplied dataset does not include in vitro validation, the present results should be considered as prioritising hypotheses rather than proof of biological activity.

Practical implications and next steps

The findings nominate C7 and C11 for prioritised follow-up. Recommended next steps are: [1] redocking the native crystal ligand to validate the docking protocol and to report an RMSD; [2] rescoring top poses using MM-GBSA; [3] performing short (50–100 ns) MD simulations on C7–ERα and C11–ERα complexes to confirm pose stability and to compute time-averaged interaction fingerprints; [4] running in-silico ADME/Tox filters to screen for drug-likeness and synthetic feasibility; and [5] advancing experimentally via binding assays and cell-based antiproliferative screens if computational profiles are favourable (8, 9, 20). These steps will move the candidates from computational hypotheses to experimentally validated leads.

Study limitations

The present analysis has several limitations that should be acknowledged. First, the molecular docking workflow relied on a single docking engine and scoring function. While this approach provides an initial indication of ligand–protein binding affinity and orientation, the absence of consensus scoring from multiple docking platforms may limit the robustness of the predicted binding interactions. Different docking algorithms and scoring functions often produce variable estimates of binding affinity; therefore, integrating multiple computational tools could improve the reliability of the predictions.

Second, the study did not incorporate molecular dynamics (MD) simulations or free energy perturbation analyses. Such approaches are increasingly used in computational drug discovery to assess the stability of ligand–protein complexes over time and to provide more accurate estimates of binding free energies. Without these dynamic simulations, the current findings are restricted to static docking poses and may not fully capture the conformational flexibility of the receptor–ligand system.

Third, the dataset did not include experimental biological validation of the predicted inhibitory activity. Consequently, the results remain computational predictions that require confirmation through in vitro or in vivo assays. Experimental evaluation, such as enzyme inhibition studies, cell-based assays, or structure–activity relationship analyses, would be essential to substantiate the therapeutic potential of the identified benzimidazole derivatives.

Taken together, these limitations highlight the need for further computational refinement and experimental validation to strengthen the translational relevance of the findings.

Conclusion

Within the constraints of a docking-only computational workflow and using the authors' DFT-optimised structures, benzimidazole derivatives C7 and C11 show the most favourable predicted binding to mutant ERα. They combine directional hydrogen bonds with dense hydrophobic and aromatic interactions that stabilise binding. These molecules are recommended for prioritised computational refinement (redocking, rescoring, MD) and subsequent experimental testing to confirm biological activity.

List of Abbreviations

AM1: Austin Model 1
B3LYP: Becke-3-parameter-Lee–Yang–Parr functional
DFT: Density Functional Theory
Erα: Oestrogen receptor alpha
MD: Molecular dynamics
MM-GBSA: Molecular mechanics generalised Born surface area
MOE: Molecular Operating Environment
PDB: Protein Data Bank
RMSD: Root mean square deviation.

Declarations

Ethics approval and consent to participate
Not applicable; no human participants or animals were used.

Consent for publication
All authors gave consent for publication under the Creative Commons Attribution Non-Commercial 4.0 license.

Data availability
The datasets generated and analysed during the current study (optimised structures, docking input files and pose outputs) are available from the corresponding author on reasonable request.

Competing interests
The authors declare no competing interests.

Funding
No external funding was reported for the computational work described in the supplied dataset.

Author contributions
NMN: Conceptualisation, ligand design and DFT optimisation.
KAH: Docking execution, interaction analysis and data curation.
EMO: Supervision, methodology refinement and manuscript editing.
All authors approved the final manuscript.

Acknowledgements
The authors thank colleagues in the Department of Chemistry, University of Anbar, for feedback during dataset preparation and Ms/Mr X for assistance with software licences. The original manuscript files supplied formed the basis for this restructured and expanded submission.

References

1. Jemal A, Bray F, Center MM, Ferlay J, Ward E, Forman D. Global cancer statistics. CA: a cancer journal for clinicians. 2011 Mar;61(2):69-90. https://doi.org/10.3322/caac.20107
2. Careaga VP, Maier MS. Cytotoxic triterpene glycosides from sea cucumbers. InHandbook of anticancer drugs from marine origin 2014 Nov 28 (pp. 515-528). Cham: Springer International Publishing. https://doi.org/10.1007/978-3-319-07145-9_24
3. Ferlay J, Shin HR, Bray F, Forman D, Mathers C, Parkin DM. GLOBOCAN v1. 2, Cancer Incidence and Mortality Worldwide: IARC Cancer Base No. 10 [Internet]. Lyon, France: International Agency for Research on Cancer; 2010 [Internet]. 2008
4. Mareel M, Leroy A. Clinical, cellular, and molecular aspects of cancer invasion. Physiological reviews. 2003 Apr 1;83(2):337-76. https://doi.org/10.1152/physrev.00024.2002
5. Wesche J, Haglund K, Haugsten EM. Fibroblast growth factors and their receptors in cancer. Biochemical Journal. 2011 Jul 15;437(2):199-213. https://doi.org/10.1042/BJ20101603
6. Vardatsikos G, Sahu A, Srivastava AK. The insulin-like growth factor family: molecular mechanisms, redox regulation, and clinical implications. Antioxidants & redox signaling. 2009 May 1;11(5):1165-90. https://doi.org/10.1089/ars.2008.2161
7. Bhat AA, Tandon N, Tandon R. Pyrrolidine derivatives as Anti-diabetic agents: Current status and future prospects. ChemistrySelect. 2022 Feb 11;7(6):e202103757. https://doi.org/10.1002/slct.202103757
8. Vijayaraghavalu S, Peetla C, Lu S, Labhasetwar V. Epigenetic modulation of the biophysical properties of drug-resistant cell lipids to restore drug transport and endocytic functions. Molecular pharmaceutics. 2012 Sep 4;9(9):2730-42. https://doi.org/10.1021/mp300281t
9. Bhat AA, Singh I, Tandon N, Tandon R. Structure activity relationship (SAR) and anticancer activity of pyrrolidine derivatives: Recent developments and future prospects (A review). European Journal of Medicinal Chemistry. 2023 Jan 15;246:114954. https://doi.org/10.1016/j.ejmech.2022.114954
10. Sachdeva H, Khaturia S, Saquib M, Khatik N, Khandelwal AR, Meena R, Sharma K. Oxygen-and sulphur-containing heterocyclic compounds as potential anticancer agents. Applied Biochemistry and Biotechnology. 2022 Dec;194(12):6438-67. https://doi.org/10.1007/s12010-022-04099-w
11. Amin A, Qadir T, Sharma PK, Jeelani I, Abe H. A review on the medicinal and industrial applications of N-containing heterocycles. The Open Medicinal Chemistry Journal. 2022 Nov 16;16(1). https://doi.org/10.2174/18741045-v16-e2209010
12. Negi B, Kwatra A. A review of recent progress on the anticancer activity of heterocyclic compounds. SynOpen. 2024 Sep;8(03):185-210. https://doi.org/10.1055/s-0040-1720125
13. Valdez J, Cedillo R, Hernandez-Campos A, Yepez L, Hernandez-Luis F, Navarrete-Vazquez G, Tapia A, Cortes R, Hernández M, Castillo R. Synthesis and antiparasitic activity of 1H-benzimidazole derivatives. Bioorganic & Medicinal Chemistry Letters. 2002 Aug

19;12(16):2221-4. https://doi.org/10.1016/S0960-894X(02)00346-3
14. Abdelrazek FM, Zaki ME, Al-Hussain SA, Farag B, Hebishy AM, Abdelfattah MS, Hassan SM, El-Farargy AF, Iovkova L, Mross D, Gomha SM. Facile one-pot synthesis and in silico study of new heterocyclic scaffolds with 4-pyridyl moiety: Mechanistic insights and X-ray crystallographic elucidation. Heliyon. 2024 Apr 15;10(7). https://doi.org/10.1016/j.heliyon.2024.e29221
15. Debus, H.: On the effect of ammonia on glyoxal. Justus Liebig's Annals of Chemistry. 1858; 107(2):199-208. https://doi.org/10.1002/jlac.18581070209
16. Satija G, Sharma B, Madan A, Iqubal A, Shaquiquzzaman M, Akhter M, Parvez S, Khan MA, Alam MM. Benzimidazole based derivatives as anticancer agents: Structure activity relationship analysis for various targets. Journal of Heterocyclic Chemistry. 2022 Jan;59(1):22-66. https://doi.org/10.1002/jhet.4355
17. Ranjith R. The chemistry and biological significance of imidazole, benzimidazole, benzoxazole, tetrazole and quinazolinone nucleus. J. Chem. Pharm. Res. 2016;8(5):505-26.
18. Othman DI, Hamdi A, Tawfik SS, Elgazar AA, Mostafa AS. Identification of new benzimidazole-triazole hybrids as anticancer agents: multi-target recognition, in vitro and in silico studies. Journal of Enzyme Inhibition and Medicinal Chemistry. 2023 Dec 31;38(1):2166037. https://doi.org/10.1080/14756366.2023.2166037
19. Nawareg NA, Mostafa AS, El-Messery SM, Nasr MN. New benzimidazole based hybrids: synthesis, molecular modeling study and anticancer evaluation as TopoII inhibitors. Bioorganic Chemistry. 2022 Oct 1;127:106038. https://doi.org/10.1016/j.bioorg.2022.106038
20. Sović I, Jambon S, Pavelić SK, Markova-Car E, Ilić N, Depauw S, David-Cordonnier MH, Karminski-Zamola G. Synthesis, antitumor activity and DNA binding features of benzothiazolyl and benzimidazolyl substituted isoindolines. Bioorganic & medicinal chemistry. 2018 May 1;26(8):1950-60. https://doi.org/10.1016/j.bmc.2018.02.045
21. Sheng C, Miao Z, Zhang W. New strategies in the discovery of novel non-camptothecin topoisomerase I inhibitors. Current medicinal chemistry. 2011 Oct 1;18(28):4389-409. https://doi.org/10.2174/092986711797200453
22. Galal SA, Hegab KH, Hashem AM, Youssef NS. Synthesis and antitumor activity of novel benzimidazole-5-carboxylic acid derivatives and their transition metal complexes as topoisomerease II inhibitors. European journal of medicinal chemistry. 2010 Dec 1;45(12):5685-91. https://doi.org/10.1016/j.ejmech.2010.09.023
23. Noha RM, Abdelhameid MK, Ismail MM, Mohammed MR, Salwa E. Design, synthesis and screening of benzimidazole containing compounds with methoxylated aryl radicals as cytotoxic molecules on (HCT-116) colon cancer cells. European Journal of Medicinal Chemistry. 2021 Jan 1;209:112870. https://doi.org/10.1016/j.ejmech.2020.112870
24. (Software reference) ChemDraw Ultra 12.0. Available from: https://chemdraw-pro.software.informer.com/12.0/.
25. Gray M, Bowling PE, Herbert JM. Comment on “Benchmarking basis sets for density functional theory thermochemistry calculations: why unpolarized basis sets and the polarized 6-311G family should be avoided”. The Journal of Physical Chemistry A. 2024 Aug 27;128(36):7739-45. https://doi.org/10.1021/acs.jpca.4c00283
26. Zhan Y, Wang Y, He S, Zhu H, Guo H, Sun H, Liu M. Design, Synthesis, Biological Evaluation and Molecular Docking Studies of 5-fluorouracil-dithiocarbamate Conjugates. Letters in Drug Design & Discovery. 2024 May 1;21(6):1120-36. https://doi.org/10.2174/1570180820666230203113746
27. Aertgeerts K, Skene R, Sogabe S. HER2 kinase domain complexed with TAK-285. Protein Data Bank; PDB ID: 3RCD. Released 2011. https://doi.org/10.2210/pdb3rcd/pdb